ISBN: 978-3-95450-227-1 ISSN: 2673-5490 doi:10.18429/JACoW-IPAC2022-THPOPT066

HELICAL WIGGLER DESIGN FOR OPTICAL STOCHASTIC COOLING AT CESR*

V.A. Khachatryan[1†], M.B. Andorf[1], I.V. Bazarov[1], W.F. Bergan[2], J.A. Crittenden[1], S.J. Levenson[1], J.M. Maxson[1], D.L. Rubin[1], J.P. Shanks[1], S.T. Wang[1]
[1]CLASSE, Cornell University, Ithaca, NY, USA
[2] Brookhaven National Laboratory, Upton, NY, USA

Abstract

A helical wiggler with parameter K_{und} = 4.35 has been designed for the Optical Stochastic Cooling (OSC) experiment in the Cornell Electron Storage Ring (CESR). We consider four Halbach arrays, which dimensions are optimized to get the required helical field profile, as well as, to get the best Dynamic Aperture (DA) in simulations. The end poles are designed with different dimensions to minimize the first and second field integrals to avoid the need of additional correctors for the beam orbit. The design is adapted to minimize the risk of demagnetization of the magnet blocks. To quantify the tolerances, we simulated the effects of different types of geometrical and magnetic field errors on the OSC damping rates. In addition, to understand the challenges for the construction, as well as, to validate the model field calculations, a prototype wiggler with two periods has been constructed. The prototype field is compared to the model, and the results are presented in this work.

INTRODUCTION

Optical Stochastic Cooling is considered one of the most promising methods for cooling stored particle beams. A key aspect of OSC is a pair of wigglers. The so called pickup wiggler radiates at optical frequencies. The kicker wiggler couples the radiation emitted by the pickup back into the beam at a phase that effects cooling. The idea was proposed in 1993 by A.A. Mikhailichenko and M.S. Zolotorev [1] and later refined by Zololotorev and Zholents into transit time OSC [2]. A high gain OSC demonstration in the Cornell Electron Storage Ring is an experimental aimed at developing.

For the demonstration of OSC at CESR the plan is to use a pair of identical helical wigglers for pickup and kicker. For compatibility with an optical amplifier based on a Ti:Sapphire gain medium, the wigglers are designed to radiate at a wavelength of 780 nm, corresponding to parameter K_{und}=4.35 for a beam energy of 1 GeV. The energy kick in the 14-period long kicker, which is the result of the interaction between the radiated wave-packet and the electron beam, is estimated to be 420 meV. The details about OSC simulations at CESR can be found in articles [3–5]. The focus of this work is the design of the wigglers based on permanent magnets. Nowadays, widely available Neodymium magnets give excellent opportunity to build more affordable wigglers compared to similar electromagnets, which have more complicated geometry, need separate power supplies and cooling subsystems.

HELICAL WIGGLER DESIGN

The configuration of magnetic material and shaping steel that generates a helical magnetic field has been defined and demonstrated. The dimensions of the components have been optimized for field quality. The end poles have been modified to tune the fringe fields. In addition, dependencies on geometrical errors and temperature variation have been investigated. Calculation of the forces between the magnet-steel arrays have been completed.

The coordinate system: Z axis is the beam direction, X and Y axes are horizontal and vertical directions respectively.

Geometry and Magnet Definition The wiggler geometry and the following field calculations are performed using the OPERA3D package [6]. The idea is to define four Halbach hybrid arrays [7] (top-left, top-right, bottom-left and bottom right), which can form two planar wigglers diagonally (top-left with bottom right, and top-right with bottom-left). The helical field can be achieved by giving a quarter period offset to one of the diagonal combination (see Fig. 1). As for magnet blocks, the best choice for such projects are Neodymium Ferrite Boron (NdFeB) magnets, as those are the strongest type of permanent magnets available commercially.

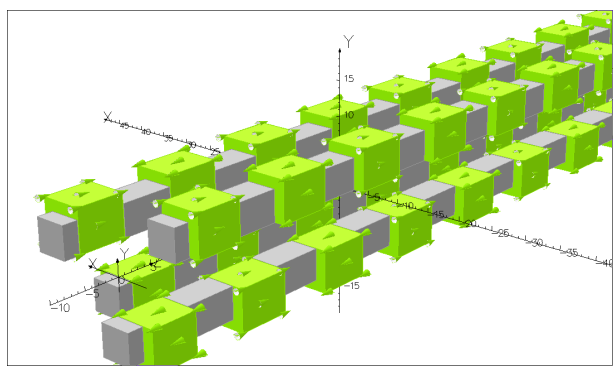

Figure 1: Permanent magnet based helical wiggler Opera-3D model. The green blocks are magnet blocks, the arrows show their magnetization orientation, the gray blocks are steel.

* Work supported by NSF award PHY-1549132 and DGE-1650441
† vk348@cornell.edu

ISBN: 978-3-95450-227-1 ISSN: 2673-5490 doi:10.18429/JACoW-IPAC2022-THPOPT066

The magnetic field horizontal and vertical components are fitted with the following functions simultaneously.

$$\begin{cases} f_x(z) = A \times \sin(kz + \phi) + f'_x(z) \\ f_y(z) = A \times \cos(kz + \phi) + f'_y(z) \end{cases} \quad (1)$$

where A, k and ϕ are fit parameters and they are the same for both $f_x(z)$ and $f_y(z)$. The functions $f'_x(z)$ and $f'_y(z)$ are responsible for higher - 3rd, 5th and 7th harmonics, with amplitudes typically at least an order of magnetic smaller (than the fundamental) in the models we studied and play a negligible role in the OSC process. The Root [8] package and Minuit::Migrad [9] minimization method are used for the magnetic field profile analyses. An example of the model field and a field profile fit can be seen on Fig 2.

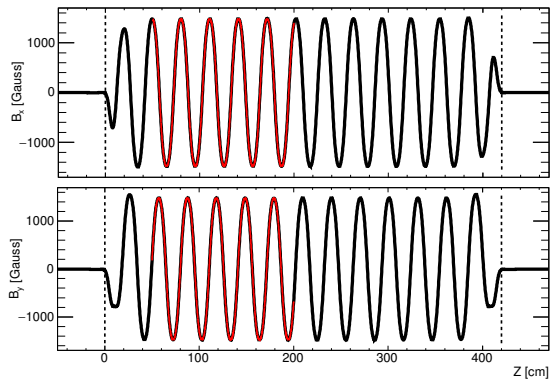

Figure 2: Field profile from Opera3D model. The black curve is the model field, and the red one is a fit with $f_{x,y}(z)$ and $f'_{x,y}(z)$ functions. The field amplitude in this model is 1550 Gs, the 3rd, 5th and 7th harmonics are 74.9 Gs, 4.2 Gs, and 1.27 Gs respectively. Dashed black lines show the start and end of the 14-period wiggler. The top and bottom figures correspond to horizontal and vertical planes respectively.

The B-H curves for the definition of different types of NdFeB-Neodymium magnets (N-35, N-43, N-52) are taken from K&J Magnetics data base [10].

Geometry and Field Optimization The aim of this study is obtaining the required magnetic field profile and simultaneously minimizing the dimensions of the magnet and steel blocks, and making the design more compact.

A smaller wiggler gap generates a higher field amplitude, thereby requiring smaller magnet blocks. However, the minimum gap size is set by vertical dimension of the CESR vacuum pipe of approximately 5 cm. An additional 0.8cm is introduced to allow for fine tuning of the magnetic field. Studies show that the maximum flux can be achieved by reducing the steel transverse (X-Y) dimensions by 25% in each plane, while the inner distance between the steel blocks has to remain the same as for magnet blocks (Fig. 1).

Reduction of the length of the steel blocks, and expansion of the length of the magnet blocks also helps to increase the magnetic field amplitude. For example 5:1 ratio for magnet:steel length makes the flux higher by about 20%. However, BMAD [11] simulations show that the best Dynamic Aperture is obtained for magnet:steel length ratio 1:1.

The model field amplitude with Neodymium N-52 magnet blocks is 10% stronger compared to the same model field amplitude with N-42 magnets, and 18% stronger compared to the model with N-35 magnets. Thus, the wiggler with Neodymium N-52 magnets can be more compact.

The optimal dimensions for the OSC wiggler: the magnet blocks need to have 2.3" (5.842 cm) square profile transversely and ~3" (7.5 cm) length. The distance between the arrays are 2.3" (5.842 cm). Neodymium N-52 magnet blocks are chosen for the above geometry. The steel blocks have the same length (7.5 cm), but the width and height are 4.38 cm, smaller by the factor of 0.75 compared to the magnet blocks.

Corrections for the Fringe Field One of the challenges of such a wiggler design is its end geometry. Ideally the first and second field integrals are zero, in other words the beam transverse momentum at the exit from the wiggler must be zero and the beam oscillation axis inside the wiggler must be parallel to the initial beam axis. The first order of Runge-Kutta tracking has been used for this study and for the wiggler design optimization [12]. We optimize the fringe field profile by varying the lengths of the last magnet and steel blocks separately. This is a 2D scan. For the geometry discussed in the previous paragraph, the first and last magnet blocks of the arrays must be 6.25 cm long and the steel blocks 2.25 cm long (see Fig. 1). Figure 3 shows 1 GeV e^- beam tracking in the model magnetic field. It is worth mentioning that CESR steerings are available at the proposed location of the wigglers, so relatively small kicks due to the fringe fields (a few hundreds of μrad kicks) can be corrected by the CESR steerings.

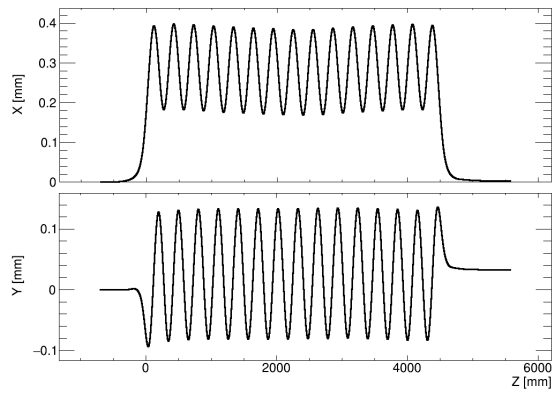

Figure 3: 1 GeV electron beam trajectory simulation in the wiggler model field. The top and bottom figures correspond to horizontal and vertical planes respectively.

Geometrical Errors The impact of geometrical errors on the field profile has been studied. Local block displace-

ISBN: 978-3-95450-227-1 ISSN: 2673-5490 doi:10.18429/JACoW-IPAC2022-THPOPT066

ments by several millimeters, or overall bends and waves with amplitudes of millimeters were considered in the model. We believe that 1 mm deviation from the design geometry is an overestimate of construction tolerances. The studies of the models show that the above mentioned geometrical deviations bring less than 0.52%/mm errors in the model magnetic field. The model field profiles with different types of geometrical errors are used in Synchrotron Radiation Workshop (SRW) [13] simulations to estimate the impact of geometrical errors on the total kick energy, and the results are compared to the ideal (theoretical) calculations. These studies confirmed that 1 mm geometrical errors impacts are expected to be negligible on the OSC process.

In addition to geometrical errors, different composition of low carbon steels (B-H data) were used in the models. Simulations show that the OSC process is relatively insensitive to the choice of steel. Within the steel compositions S1005-S1020 and A36 [14], the largest difference is between the model fields with steel S1005 and A36. However the difference is less than 0.6% of the field amplitude.

In this document we do not discuss in details the demagnetization studies, force calculations, and the temperature sensitivity. Demagnetization risks are reduced by adding a 1 mm layer of non-magnetic materials between the magnet and steel blocks in the arrays.

The forces are calculated and there are only pulling forces between the diagonal arrays, which are estimated on the level of 2000 N. Due to the design symmetry the other forces cancel out each other.

Lastly, for the design 40^0 C B-H data are used for the definition of the Neodymium magnets. The CESR tunnel average temperature during the operation is about 30^0 C, which is lower than the wiggler's design temperature, and this will increase the field amplitude by 1.5%.

PROTOTYPING AND THE DESIGN VALIDATION

To validate the wiggler design and to better understand the construction challenges a 2 period prototype has been built with 6" period length, 2.5cm×5cm transverse dimensions for the magnets, and ~750 Gs on-axis field amplitude. The wiggler model has been adopted to the dimensions of the prototype and the field calculations are performed for the prototype geometry. All the geometrical deviations are accounted for in the prototype model with the accuracy of 0.5 mm. The Hall probes used in the magnetic field measurements have accuracy on the level 1%. The prototype, as well as, the comparison between the model field and measured prototype field can be seen on Fig. 4.

One can see that the worst disagreement between the prototype end model fields is on the level of 20 Gs, which is ~2.7% from the field amplitude. Also, the discrepancy mostly is in the fringe field region, because of magnetic materials presence in the ends of prototype construction. The next step is to improve the geometry, re-assemble the prototype without magnetic materials, implement the geometrical errors into the model with a better accuracy. However, the results are already satisfactory: the magnetic field calculations are acceptable to first order, and there are no destabilizing forces.

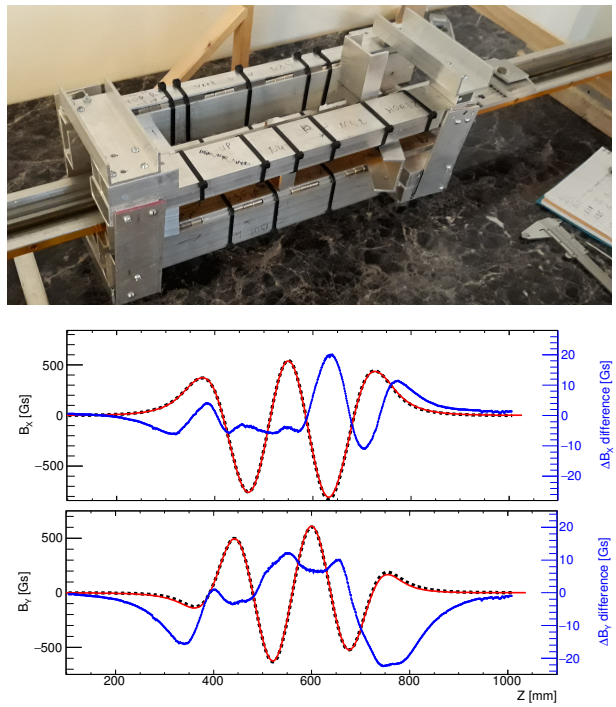

Figure 4: Prototype and model on-axis magnetic fields. The red curve on the graph is the model field, the black-dashed curve is the measured prototype field, and the blue curve is the model and prototype difference, its vertical axis is on the right side of the plot. The top and bottom figures correspond to horizontal and vertical planes respectively.

CONCLUSION

A NdFeB permanent magnet based helical wiggler has been designed. For the presented design the helical field amplitude is estimated $A = 1.55$ kGs ($K_{und} = 4.35$). The possible geometrical errors are modeled, and their impact on the magnetic field is expected to be negligible. A 1 mm gap between the magnet and steel blocks will help to avoid the demagnetization of the magnet blocks. A small 2-period prototype has been constructed and the field analyses validate the wiggler's design.

ACKNOWLEDGEMENTS

The authors want to thank David Sagan for the help with getting the wiggler model for the BMAD simulations.

We thank the Center for Bright Beams, NSF award PHY-1549132, NSF Graduate Research Fellowship Program under grant number DGE-1650441 for the support of the project.

We also thank the Monroe Engineering team for the useful discussions and quotes for custom dimensions NdFeB magnets.

ISBN: 978-3-95450-227-1 ISSN: 2673-5490 doi:10.18429/JACoW-IPAC2022-THPOPT066

REFERENCES

[1] A.A. Mikhailichenko and M.S. Zolotorev, "Optical Stochastic Cooling", *Phys. Rev. Lett.*, vol. 71, p. 4146, 1993. doi:10.1103/PhysRevLett.71.4146

[2] M.S. Zolotorev and A.A. Zholents, "Transit-time method of optical stochastic cooling", *Phys. Rev. E*, vol. 50, p. 3087, 1994. doi:10.1103/PhysRevE.50.3087

[3] W.F. Bergan *et al.*, "Bypass Design for Testing Optical Stochastic Cooling at the Cornell Electron Storage Ring (CESR)", in *Proc. IPAC'19*, Melbourne, Australia, May 2019, pp. 360–363. doi:10.18429/JACoW-IPAC2019-MOPGW100

[4] M. B. Andorf *et al.*, "Optical stochastic cooling with an arc bypass in the Cornell Electron Storage Ring", *Phys. Rev. Accel. Beams*, vol. 23, p. 102801, 2020. doi:10.1103/PhysRevAccelBeams.23.102801

[5] S. T. Wang *et al.*, "Simulation of the transit-time optical stochastic cooling process in the Cornell Electron Storage Ring", *Phys. Rev. Accel. Beams*, vol. 24, p. 064001, 2021. doi:10.1103/PhysRevAccelBeams.24.064001

[6] Opera Simulation Software Suite. https://www.3ds.com/products-services/simulia/products/opera/

[7] K. Halbach, "Physical and optical properties of rare earth cobalt magnets", *Nuclear Instruments and Methods*, vol. 187, pp. 109-117, 1981. doi:10.1016/0029-554X(81)90477-8

[8] ROOT Data Analysis Framework, https://root.cern.ch/

[9] F. James, "Function Minimization and Error Analysis", CERN program library writeup D506, 1998, https://cds.cern.ch/record/2296388/files/minuit.pdf/

[10] K&J Magnetics, Inc. Demagnetization (BH) Curves for Neodymium Magnets, https://www.kjmagnetics.com/bhcurves.asp/

[11] D. Sagan, "Bmad: A relativistic charged particle simulation library", *Nucl. Instrum. Methods Phys. Res. A*, vol. 558, p. 356, 2006. doi:10.1016/j.nima.2005.11.001

[12] W.F. Bergan *et al,*, "Helical Wiggler Model for Fast Tracking", in *Proc. IPAC'19*, Melbourne, Australia, May 2019, pp. 3356–3359. doi:10.18429/JACoW-IPAC2019-WEPTS102

[13] O. Chubar, P. Elleaume, "Accurate and Efficient Computation of Synchrotron Radiation in the Near Field Region", in *Proc. EPAC'98*, Stockholm, Sweden, Jun. 1998, paper THP01G, pp 1117-1119.

[14] Magnetic Material Data,https://www.magweb.us/